Carbohydrate Polymers 156 (2017) 380–389

Contents lists available at ScienceDirect

Carbohydrate Polymers

journal homepage: www.elsevier.com/locate/carbpol

Synthesis, characterization and modification of Gum Arabic microgels for hemocompatibility and antimicrobial studies

Muhammad Farooq[a], Selin Sagbas[b,c], Mehtap Sahiner[d], Mohammad Siddiq[a], Mustafa Turk[e], Nahit Aktas[f], Nurettin Sahiner[b,c,*]

[a] Department of Chemistry, Quaid-i-Azam University, Islamabad 45320, Pakistan
[b] Faculty of Science & Arts, Chemistry Department, Canakkale Onsekiz Mart University, Terzioglu Campus, 17100 Canakkale, Turkey
[c] Nanoscience and Technology Research and Application Center (NANORAC), Canakkale Onsekiz Mart University, Terzioglu Campus, 17100 Canakkale, Turkey
[d] Leather Engineering Department, Ege University, Bornova, Izmir, 35080, Turkey
[e] Kirikkale University, Bimomedical Engineering, 06450 Kirikkale, Turkey
[f] Chemical Engineering Department, Yuzuncu Yil University, Campus, Van, 65080, Turkey

ARTICLE INFO

Article history:
Received 29 June 2016
Received in revised form 3 September 2016
Accepted 15 September 2016
Available online 16 September 2016

Keywords:
Gum Arabic microgels/nanogels
Modifiable GA particle
Degradable/biocompatible GA microgel
Antimicrobial GA microgel

ABSTRACT

Gum Arabic (GA) microgels were successfully prepared via reverse micellization method with high yield (78.5 ± 5.0%) in 5–100 μm size range using divinyl sulfone (DVS) as a crosslinker. The GA microgels were degraded hydrolytically 22.8 ± 3.5% at pH 1 in 20 days, whereas no degradation was observed at pH 7.4 and pH 9 at 37 °C. By using diethylenetriamine (DETA), and taurine (TA) as chemical modifying agents, GA microgels were chemically modified as GA-DETA and GA-TA, and the zeta potential values of 5.2 ± 4.1 and −24.8 ± 1.3 mV were measured, respectively in comparison to −27.3 ± 4.2 mV for GA. Moreover, blood compatibility of GA, GA-TA, and GA-DETA microgels was tested via *in vitro* protein adsorption, % hemolysis ratio, and blood clotting index. All the microgels were hemocompatible with% hemolysis ratio between 0.23 to 2.05, and the GA microgels were found to be highly compatible with a blood clotting index of 81 ± 40. The biocompatibility of GA, GA-DETA and GA-Taurine microgels against L929 fibroblast cells also revealed 84.4, 89.1, and 67.0% cell viability, respectively, at 25.0 μg/mL concentration, suggesting great potential in vivo biomedical applications up to this concentration. In addition, 5 and 10 mg/mL minimum inhibition concentrations of protonated GA-DETA microgels (GA-DETA-HCl) were determined against *E. coli* and *S. aureus*, respectively.

1. Introduction

Biopolymers obtained from polysaccharides are preferred for use in many biomedical applications such as high cytocompatibility and ability to degrade in body without releasing harmful substances (Ciofani et al., 2014). But still majority of biopolymers lack some essential properties like biocompatibility and mechanical stability in aqueous environments (Oh, Lee, & Park, 2009). It is of critical importance to know about the hemocompatibility and biodegradability of any material to be used *in vitro* and/or *in vivo* for biomedical applications. Various attempts such as; cross linking, breaking of the polymer chains and surface modification can be performed to achieve relative stability and desired goals from biomaterials (de las Heras Alarcón, Pennadam, & Alexander, 2005).

Natural gums are a large classification of carbohydrates with a wide range of applications especially in food, pharmaceuticals, cosmetics, adhesive, paper, textile, and other industries for centuries. The oldest and most common GA was introduced into Europe through various Arabian ports, so it was called Gum Arabic (Phillips & Williams, 2001). During the middle ages, the trade of GA was governed by the Ottoman Empire, giving rise to the name turkey gum (Verbeken, Dierckx, & Dewettinck, 2003). GA is a polydispersed molecule including a compact arabinogalactan molecule consisting of amino acids linked to short arabinose side chains (An et al., 2013). It is safe, non-digestible food element which is widely used in food and pharmaceutical industries. Positive effects linked to renal or hepatic failure are claimed by various authors (Ali, Ali, Fadlalla, & Khalid, 2008). Blocks of highly branched carbohydrates are linked to the polypeptide chain leading to a wattle blossom structure

* Corresponding author at: Nanoscience and Technology Research and Application Center (NANORAC), Canakkale Onsekiz Mart University, Terzioglu Campus, 17100 Canakkale, Turkey.
E-mail address: sahiner71@gmail.com (N. Sahiner).

http://dx.doi.org/10.1016/j.carbpol.2016.09.052
0144-8617/

(Poologanathan & Mahendran, 2012). In soft drinks it works as an emulsifier and assists as an efficient encapsulating agent for flavor where it offers a high protection from unstable flavor compounds (Romo-Hualde, Yetano-Cunchillos, González-Ferrero, Sáiz-Abajo, & González-Navarro, 2012; Verbeken et al., 2003). GA is also used in oral or topical application due to its suspending and emulsifying nature. It is used as an ingredient in pastilles, lozenges or as a binder in tablet manufacturing (Bhardwaj, Kanwar, Lal, & Gupta, 2000). The most important application of Gum Arabic is its use as a release modifier (Malviya, Jain, & Malviya, 2010).

Crosslinking of the linear chains of GA can adapt to a spherical shape enabling many applications by providing a surface which reduces degradation, is suitable for many catalytic reactions like degradation of harmful industrial effluents and reduction of poisonous metals and may be beneficial for different cell interactions (Schmuhl, Krieg, & Keizer, 2004).

Herein, we aim to prepare non-cytotoxic, chemically modifiable, and controllable biodegradable biopolymer microgel which is more convenient and readily attainable, with much potential in biomedical use. To date, vinyl sulfone chemistry has been demonstrated to be suitable for selective modification of polysaccharides and protein residues under mild conditions (Comte, Guibaud, & Baudu, 2008; Ngah, Teong, & Hanafiah, 2011).

Gum Arabic has thoroughly been studied by many research groups to achieve targeted applications. Sarika & James synthesized GA-gelatin-aldehyde (GA-Gel-A) nanogels via inverse miniemulsion technique using sodium metaperiodate for the initial addition of aldehyde groups to the GA chains for further crosslinking with gelatine (Sarika & James, 2015). The prepared nanogel template was found to be nontoxic and used in drug delivery applications. Recently, Ganie et al. prepared GA microspheres by the introduction of acetyl groups to the polysaccharide GA for further reaction with iodine monochloride (Ganie, Ali, & Mazumdar, 2015).

Modification is a simple way to tune the properties of microgels to achieve desired goals in both environmental and biological domains. In the current study, GA microgels were prepared followed by modification with DETA and TA. The described modifiers were chosen for modification due to their individual non-cytotoxicity, biocompatibility and amine terminal groups for a constructive linking capability with a negatively charged surface (Liimatainen, Sirviö, Pajari, Hormi, & Niinimäki, 2013). TA is an organic compound with a wide range of applications in biological systems. One of its major *in vitro* application is that it forms stable conjugates with chenodeoxycholic via its terminal amino group with acid and cholic acid to form bile salts such as sodium taurochen deoxycholate and sodium taurocholate. The suitable pH of the sulfonic acid group of taurine ensures this negatively charged moiety improves the surfactant properties of the cholic acid conjugate in the intestinal environment (Irving, Hammer, Danyluk, & Klein, 1980). Dwivedi and his co-workers modified cellulose with TA for the selective absorption of gold from aqueous solution (Dwivedi, Dubey, Hokkanen, Fallah, & Sillanpää, 2014). DETA is highly reactive due to its terminal amine groups and is used as curing agent for epoxy-resins, in coordination chemistry it serves as a tridentate ligand in complexes such as $Co(dien)(NO_2)_3$ (Crayton, Zitomer, & Lambert, 1963). Recently, polyaniline (PANI) modified styrene-divinyl benzene was synthesized as Michael acceptor for direct immobilization of amino acids and amines (Erdem & Bicak, 2016). DETA has potential applications in the modification of biomaterials owing to its non-toxic nature. Sardo and his co-workers developed a simple, biocompatible and cost-effective inulin-DETA based on a small interfering RNAs (siRNA) delivery system for hepatocellular carcinoma derived cells (JHH6) (Sardo et al., 2015). Glassy carbon electrodes were modified with poly(taurine) by Wang and Chen for determination of epinephrine and dopamine with high sensitivity and selectivity.

Herein we demonstrate Michael-type addition of divinyl sulfones to crosslink the linear chains of GA for the first time. This is an attractive time saving and cost-effective methodology for the synthesis of GA microgels that can be prepared at room temperature. Vinyl sulfone chemistry was demonstrated to be suitable for selective modification of proteins and carbohydrate residues under mild conditions (Jegelka & Plietker, 2012; Mather, Viswanathan, Miller, & Long, 2006; Morales-Sanfrutos et al., 2010). The GA microgels were modified with DETA and TA to tune their properties in the desired direction in biomedical domain to provide great advantages in many respects such as surface charge, biocompatibility and new functionality as well as bactericidal properties. Environmental variables such as temperature, pH, and ionic strength of water can affect the hydrolytic degradation pattern of polymers (Sahiner, Sagbas, & Aktas, 2016). Hydrolytic degradation profiles of GA microgels were determined at pH 1 (stomach conditions), pH 7.4 (blood and body fluid conditions), and pH 9 (intestinal conditions) at 37.5 °C by using high performance liquid chromatography (HPLC). Discretely, GA is a non-toxic and biocompatible natural polymer which can be used readily for food, medicinal, and pharmaceutical applications. After crosslinking and modification reactions, biocompatibility could vary associated with the additive materials. Hemocompatible materials in contact with blood should not induce mechanisms of platelet activation, thrombus formation, cell disruption, and blood coagulation (Venault, Trinh, & Chang, 2016). Therefore, the hemocompatibility of GA-based microgels was investigated through the quantity of protein adsorbed, determination of percent hemolysis ratio and blood clotting index tests *in vitro* for its potential usefulness in intravascular applications. In addition, biocompatibility of GA-based microgels was determined by performing WST-1 cytotoxicity test on L929 fibroblast cells. The non-cytotoxicity, biocompatibility and the high quantitative yields of the product GA microgels is the main focus of this study.

2. Materials and method

2.1. Materials

Gum Arabic from the Acacia tree (Branched polysaccharide, Sigma-Aldrich, Mw: 250,000 g/mol), divinyl sulfone (DVS, 98%, Merck) as chemical cross-linker, sodium bis(2-ethylhexyl) sulfosuccinate (AOT, 98%, Sigma-Aldrich) as surfactant, gasoline (Total, 95 Octane, lead free) as solvent, and epichlorohydrine (ECH, >99% Sigma-Aldrich), diethylenetriamine (DETA, 99%, Sigma-Aldrich) and taurine (99%, Sigma-Aldrich) as chemical modifying agents were used as received. Nutrient agar (for microbiology, Merck) and nutrient broth (for microbiology, Merck) were used as microbial growth media. All the solvents; acetone (99%, BRK), ethanol (99%, Birkim) and DMF (99%, Merck) were used as received. *Escherichia coli* ATCC 8739 and *Staphylococcus aureus* ATCC 6538 strains were obtained from the Microbiology Department of the School of Medicine at Canakkale Onsekiz Mart University. Sodium bicarbonate and calcium chloride were purchased from Sigma-Aldrich. L929 fibroblast cell line, Dulbecco Modified Eagles Medium (DMEM), Fetal Bovine Serum (FBS), Penicillin-Streptomycin, Trypan Blue, and Trypsin were obtained from Sigma-Aldrich for biocompatibility studies. Propidium iodides (PI) and Ribonuclease-A, Hoechst were purchased from Serva Israil. All aqueous solutions were freshly prepared using ultra-pure distilled water 18.2 MΩ cm (Millipore-Direct Q UV3).

2.2. Synthesis of GA microgels

GA microgels were synthesized according to a previously reported method with minor modification (Ilgin et al., 2010; Sagbas,

Butun, & Sahiner, 2012). Initially, 5 g of gum arabic polymer was dissolved in 50 mL of 0.5 M NaOH solution. After stirring for 30 min, 10 mL of the prepared solution was transferred to a 500 mL reaction flask containing 300 mL sodium bis-ethylhexyl sulfosuccinate (AOT) solution in gasoline. Upon mixing for 15 min more under 1500 rpm mixing rate, 0.24 mL DVS (100% relative to the repeating units of GA molecules, and the mole ratio of polymer to cross linker was set to 1:1) was added to the mixture. Soon after the addition of the crosslinker, the color of the mixture turned turbid as an indication of particle formation. The mixture was then stirred for a total of 30 min to complete crosslinking of the polymer chains. The prepared sample was precipitated with excess amount of acetone. After complete phase separation, the oil phase was decanted, and the solid residue of GA microgels were washed and centrifuged under 35544g for 10 min twice with acetone, and twice with ethanol-water mixture (50:50 by volume), and finally with ethanol for the cleaning purpose e.g., for the removal of the surfactant molecules, DVS and non-crosslinked GA chains. Then, the obtained GA microgels were dried at 50 °C overnight in an oven, and stored in a closed container for further use.

2.3. Modification of GA microgels with DETA and TA

Following the commonly practiced methods (Ali et al., 2008; Anirudhan & Rauf, 2013), the prepared microgels were modified with DETA. For modification reaction; 0.5 g of dried GA microgels were mixed with 30 mL 0.2 M NaOH solution, initially vortexed and then stirred for 20 min. After 20 min the swollen microgels were washed with DI water and centrifuged at 35544g for 10 min. The washed swollen microgels were transferred into a 50 mL reaction flask containing 20 mL DMF followed by the inclusion of 2.0 mL epichlorohydrine (ECH). The mixture was stirred at 90 °C for 60 min at 800 rpm. After 60 min, 1.5 mL DETA was added to the stirred mixture and the stirring continued for 60 min more with the expectation of sufficient modification of the GA microgels with added DETA. Again, the modified GA microgels were firstly precipitated with excess acetone and then washed three times with ethanol-water mixture (50:50 by volume) and two times with acetone for the complete removal of the unreacted ECH and DETA molecules. The obtained DETA modified GA microgels (GA-DETA microgels) were dried at 50 °C in an oven overnight and stored in a closed container for further use.

The above mentioned method (used for modification with DETA) was also used for the modification of GA microgels with TA. Accordingly; NaOH treated 0.5 g GA microgels and 2 mL ECH were transferred into a 50 mL reaction flask containing 20 mL DMF. The mixture was stirred at 90 °C for 60 min at 800 rpm. In a separate reaction vial 0.5 g of TA was dissolved in 6 mL distilled water. After 60 min the aqueous solution of TA was added dropwise to the stirred mixture. The stirring progressed for 1 h more. Finally, the TA modified GA microgels (GA-TA) were precipitated with excess acetone and then washed thrice with ethanol-water mixture (50:50 by volume), and then twice with acetone to get rid of unreacted ECH and TA molecules. The obtained GA-TA microgels were dried at 50 °C in an oven overnight, and stored in a closed container for further use.

GA-DETA was mixed with 30 mL 2 M HCl solution for 2 h to prepare the protonated GA-DETA-HCl microgels. Thereafter, the solution was centrifuged under 35544g for 10 min and washed with DI water two times followed by washing with acetone for two times. At last, the protonated GA-DETA-HCl microgels were dried at 50 °C overnight in an oven, and stored in a closed container for further use.

2.4. Characterization of GA and modified GA microgels

2.4.1. GA microgel size analysis and zeta potential measurements

Particle size and shape of bare and modified GA microgels was visualized with an optical microscope (Olympus BX53F, Japan). The average hydrodynamic diameter of the synthesized GA microgel was determined using a dynamic light scattering (DLS) instrument (Brookhaven Ins. and Cor. 90 plus particle size analyzer). The DLS experiment was carried out employing 90° angle detector, with 35 mW solid state laser detector operating at a wavelength of 658 nm. The swollen GA based microgels were filtered with syringe filter with the pore sizes of 5 μM, and the particle sizes in the filtrate was measured with DLS. The results are average values of ten consecutive measurements with an integration time of 2.

Zeta potential measurements of GA-based microgels were conducted with Zeta-Pals Zeta Potential Analyzer BIC (Brookhaven Inst. Corp.) in deionized water.

2.4.2. FT-IR and TGA analysis of GA based microgels

Fourier Transform Infrared Spectroscopy (FT-IR) of GA-based microgels were recorded by a Perkin-Elmer FT-IR spectroscope in the spectral range 4000–650 cm^{-1} using attenuated total reflectance (ATR) at 4 cm^{-1} resolutions.

Thermal analysis of GA-based microgels were carried out using a thermo-gravimetric analyzer (SII TG/DTA 6300, Japan) to study the thermal stability of bare GA (unmodified GA) and modified GA particles. TGA was performed under nitrogen atmosphere with 100 mL/min flow rate with heating rate of 10 °C/min heating up to 900 °C.

2.4.3. Hydrolytic degradation study of GA microgels

The hydrolytic degradation of GA microgels was analyzed using Thermo Ultimate 3000 HPLC system with refractive index (RI) detector containing rezex RNM-Carbohydrate Na^+ column (5 μm, 300 mm x 7.8 mm) of phenomenex via the following the HPLC conditions: 0.5 mL/min flow rate, 65 °C temperature of column and 35 °C temperature of RI detector, 20 μL of injection volume for 30 min run time. Sulfuric acid solution (5 mM) was used as the mobile phase. For calibrations of GA, the standard buffer solutions of pH 1, 7.4, and 9 (five different concentrations) were prepared in DI water.

The hydrolytic degradation characteristics of the prepared GA microgels were tested in three buffered solutions at pHs 1, 7.4, and 9 at body temperature (37.5 °C). For this purpose, 0.1 g of dried GA microgels were placed in 40 mL buffer solutions separately at pH 1 (stomach conditions), 7.4 (blood and body fluid conditions), and 9 (intestinal conditions) with three replicates each. Thereafter, the samples were put in a water shaker-bath at 37.5 °C for degradation studies. The degradation of microgel (weight loss% of microgel) was monitored for 30 days by collecting 0.5 mL of supernatant solution every second day, and diluting with the corresponding buffer solution to 1.5 mL. All the experiments were performed in three replicates and the amount of linear GA produced from the degradation profile was determined through HPLC. For baseline correction, pure buffer solutions were used. Thereafter, GA containing buffer solutions with different concentrations was measured by the same method. Only one different peak at 7.13 min was detected for all types of buffer solutions but the peak intensity at 7.13 min was changed according to the buffer solutions. The calibration points of linear GA solution at three different buffer solutions was separately measured with five concentration of GA solution at pH 5.4, 7.4, and 9 and the amounts of degrading linear GA molecule weight loss (%) into the microgel network was calculated according to the plot of the previously designed calibration curves for linear GA solution at pH 1, pH 7.4, and pH 9.

2.5. In vitro hemocompatibility assay

The hemocompatibility assay in this investigation was approved by the Human Research Ethics Committee of Canakkale Onsekiz Mart University (KAEK-2015-13). Human whole blood was taken from healthy volunteers. The fresh blood was put into hemogram tubes containing EDTA and slowly shaken. Hemocompatibility studies were investigated by protein adsorption, hemolysis assay, and blood clotting tests in accordance with the process thoroughly explained in the literature with some modifications (Archana, Dutta, & Dutta, 2013; R. Li, Wu, & Ye, 2015; Shih et al., 2006).

2.5.1. Protein adsorption assay

Bovine Serum Albumin (BSA) was used as model protein to examine the protein adsorption behavior of the GA-based microgels. Briefly, 10 mg GA-based microgels were placed in 30 mL PBS solution at 37.5 °C for 1 h. Then, the GA microgel containing turbid solution was precipitated by centrifugation at 35544*g* for 10 min to obtain swollen microgels by discarding the supernatant. The swollen GA-based microgels were put into 30 mL 300 ppm BSA solution in PBS and incubated at 37.5 °C for 2 h. The adsorbed amount of BSA was determined by measuring the decrease in BSA concentration at 280 nm via UV–vis spectroscopy, from a calibration curve that is constructed at 280 nm for BSA solution. The overall decrease amount of BSA was calculated according to the Eq. (1):

$$\text{Proteinadsorption(mg/g)} = ((A_0 - A_t)/\text{slopeofBSAcalibration}) \times \text{amountofmicrogel(g)/volumeofBSAsolution(L)} \quad (1)$$

A_0 is the absorbance of the stock solution of BSA, A_t is the absorbance of supernatant BSA solution containing microgel after 2 h incubation. The protein adsorption test was carried out four times.

2.5.2. Hemolysis assay

For hemolytic study, a stock solution of 1 mg/mL GA-based microgel was prepared in 10 mL 0.9% saline solution. The suspension was diluted by 2, 4, and 10 fold with 0.9% saline solution and while kept at 37.5 °C. Anticoagulant containing 2 mL blood was diluted with 2.5 mL of 0.9% saline solution. Then, 0.2 mL diluted blood solution was added to 10 mL of GA microgel suspension and incubated at 37.5 °C for 1 h in a shaker bath. After the incubation, the suspensions were centrifuged at 100*g* for 5 min and the absorbance of the supernatant solutions was measured by UV–vis spectrophotometer at 542 nm for the determination of released amount of hemoglobin. The hemolysis% ratio was calculated from Eq. (2):

$$\text{Hemolysisratio\%} = (A_{\text{sample}} - A_{\text{negative}})/(A_{\text{positive}} - A_{\text{negative}}) \times 100 \quad (2)$$

Where A_{sample}, A_{positive}, and A_{negative} are the absorbance of sample-containing blood solution, 0.2 mL diluted blood in 10 mL DI water, and 0.2 mL diluted blood in 10 mL saline solution, respectively. Hemolysis tests were carried as in six replicates, and data are given as the average of these values with standard deviations.

2.5.3. Blood clotting assay

For blood clotting study, 0.24 mL 0.2 M $CaCl_2$ solution was added to 3 mL anticoagulant containing blood and kept agitated slowly. Then, 0.27 mL of this blood solution was dropped on to 10 mg of GA-based microgels into flat-bottomed tubes until all the sample was covered. The medium was incubated in a water shaker bath at 37.5 °C for 10 min. After the incubation, 10 mL DI water was slowly added into the medium and immediately centrifuged at 100*g* for 30 s. The supernatant solution was taken and diluted with 40 mL DI water. This blood medium was incubated in a shaking bath at 37.5 °C for 1 h, and the absorbance of this solution was determined by using UV–vis spectrophotometer at 542 nm. The blood clotting index was evaluated from Eq. (3):

$$\text{Bloodclottingindex} = (A_{\text{sample+blood}}/A_{\text{blood}}) \times 100 \quad (3)$$

Where $A_{\text{sample+blood}}$ and A_{blood} are the absorbance of blood solutions contacted with the sample and diluted in 50 mL DI water. Blood clotting test was repeated six times.

2.6. WST-1 cytotoxicity test and double staining for apoptosis and necrosis

Frozen cells were dissolved at 37 °C, and placed into a 15 mL falcon tube in a laminar air flow cabinet for cell culture studies. The cells were centrifuged at 2500 rpm for 2 min, and 3 mL of DMEM/F-12 (containing 10% FBS and 1% antibiotic) growth medium was added to each tube and immediately homogenized. The cells were incubated at 37 °C in a 5% CO_2 atmosphere using a 25 cm^2 flask for 24 h.

The live cells containing 2×10^4 cells were placed in 48 well plates. DMEM medium including 10% FBS and 1% penicillin streptomycin were added to the cells. The cells were incubated at 37 °C in a 5% CO_2 atmosphere for 24 h. The prepared GA-based microgel at 0, 6.25, 12.5, 25, 50, 100, and 200 μg/mL concentrations were treated with the cells and incubated for 24 h. Then, the dead cells were removed and fresh medium was added. For each well, 7.5 μL of WST-1 (water soluble tetrazolium salt) reagent was added and incubated for 4 h. The plates were measured with an Elisa Microplate Reader (BioTek, USA) at 440 nm wavelength. Every assay was repeated three times.

Apoptosis and necrosis of L929 fibroblast cells were determined by the double staining method. Briefly, the live cells containing 2×10^4 cells were placed in 48 well plates. DMEM medium including 10% FBS and 1% penicillin streptomycin was added to the cells. The cells were incubated at 37 °C in a 5% CO_2 atmosphere for 24 h. The prepared GA-based microgel at 0, 6.25, 12.5, 25, 50, 100, and 200 μg/mL concentrations were treated with the cells and incubated for 24 h. Double staining solution was prepared with Hoechst dye 33342 (500 μL), propidium iodide (PI, 100 μL) and DNAse free-RNAse (100 μL) dissolved in 10 mL PBS. After the incubation, the dead cells were removed, and 70 μL of double staining solution was dropped in each well and left for 15 min in the dark. The apoptotic and necrotic cells were counted by using a DMI600 Fluorescence Inverted Microscope (Leica, Germany) with DAPI and FITC filters.

2.7. Antimicrobial properties of GA, GA-DETA and GA-TA microgels

Antimicrobial effects of GA-based particles were determined with broth-micro dilution tests against gram-negative *Escherichia coli* ATCC 8739 (Gram −) and *Staphylococcus aureus* ATCC 6538 (Gram +) bacteria strains. Stock cultures were revived in nutrient broth (NB) at 35 °C for 24 h to adjust to approximately 100×10^7 colony forming unit per mL (CFU mL^{-1}). For sterilization, microgels were irradiated for 5 min under 420 nm UV light. Separately, 100, 50, 25, and 10 mg sterile microgels were dispersed in 9.9 mL Nutrient Broth, and 0.1 mL bacteria culture was added to Nutrient Broth medium at 35 °C for 18–24 h of incubation time. Then, 100 μL of culture medium was inoculated on nutrient agar and incubated for 18–24 h at 35 °C. The growing colonies were detected on agar plate. Minimum inhibition concentration (MIC) values of GA-based microgels were determined as the minimum concentration of antimicrobial material at which no turbidity (visible growth) was observed in Nutrient Broth culture medium.

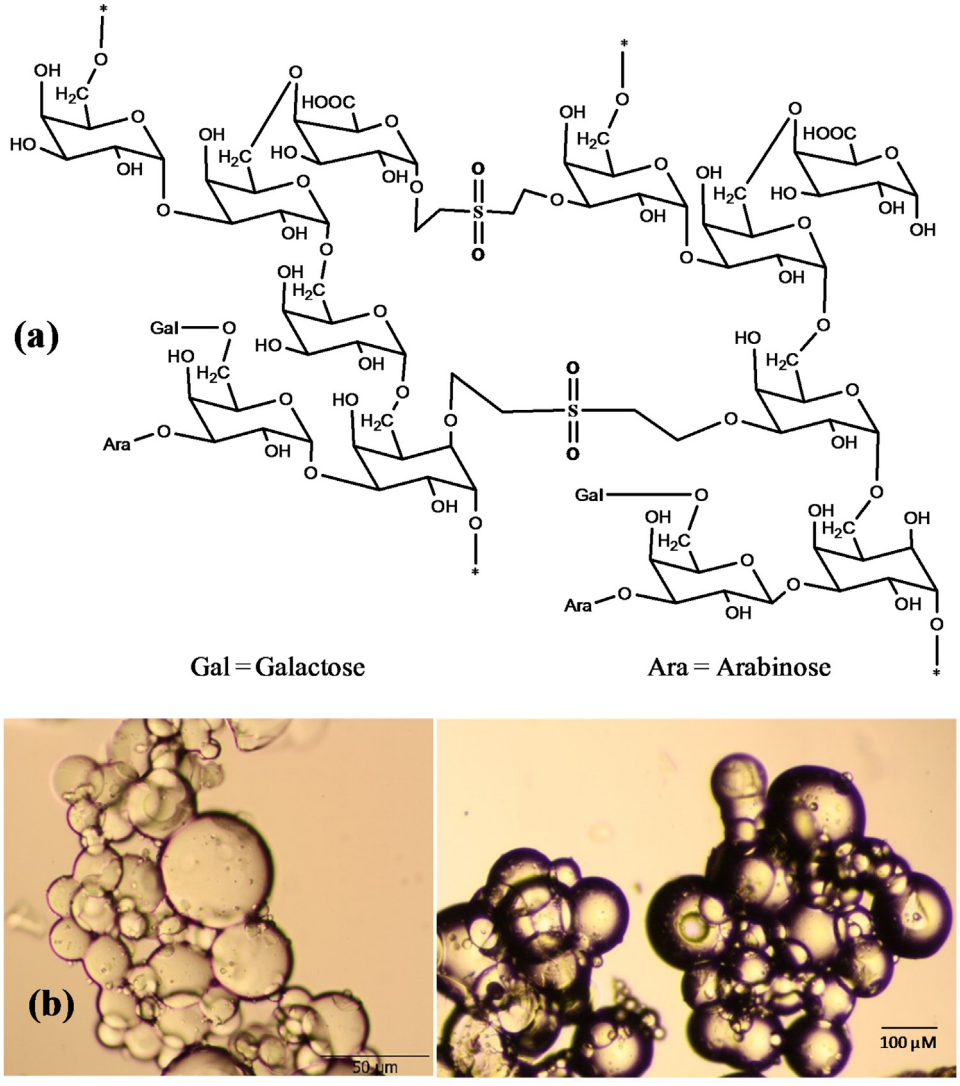

Fig. 1. (a) Schematic representation of crosslinking of GA chains by DVS crosslinker and (b) optical microscope image of GA microgels.

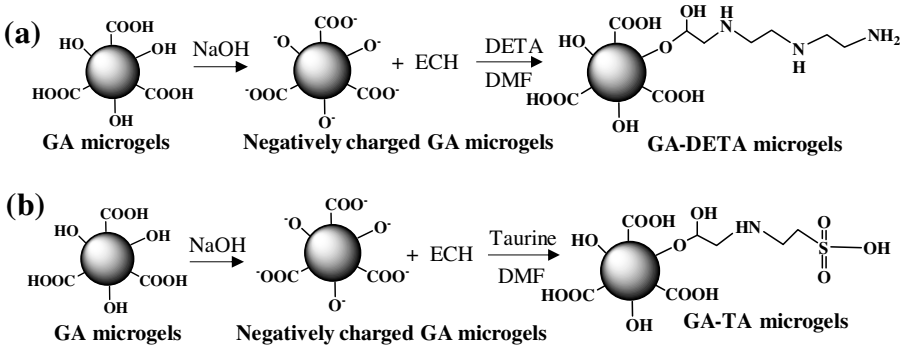

Fig. 2. Schematic representation of modification of GA microgels by (a) DETA and (b) TA.

3. Results and discussion

3.1. Synthesis, modification, and characterization of GA-based microgels

Here, a simple approach for the synthesis of GA microgels by crosslinking GA chains with DVS in AOT microemulsion system with a high yield of 78.5 ± 5.0% is presented. Hydrophilic GA polymer resides in the reverse micelles core of the AOT microemulsion system (Ekici, Ilgin, Butun, & Sahiner, 2011; Sahiner, Sagbas, & Turk, 2014). Upon addition of DVS under constant stirring they diffuse inside the micro emulsion and react with the hydroxyl groups of different chains, e.g., amongst the any monosaccharide residue, intra-, and inter-chains of GA

via Michael addition type reaction forming GA microgels (Oh et al., 2009; Sagbas et al., 2012; Sahiner & Xinqiao, 2008). Fig. 1a

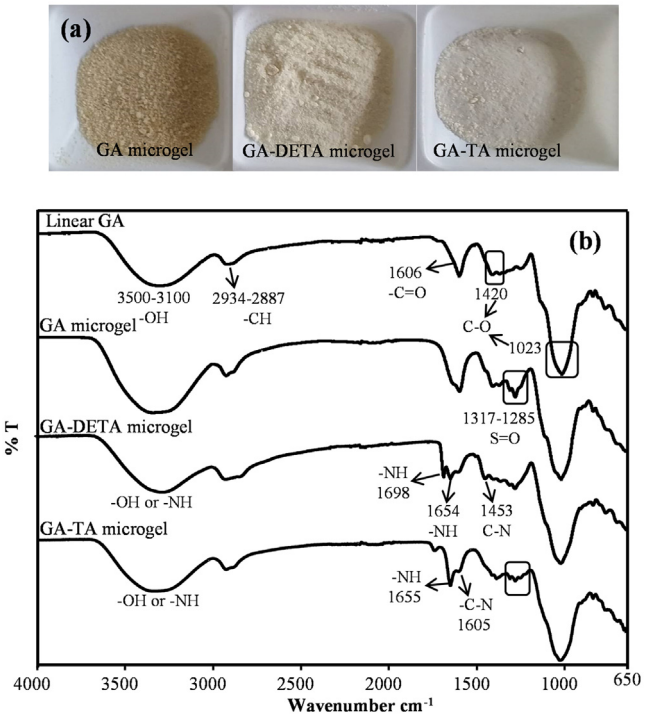

Fig. 3. (a) Digital camera images of GA, GA-DETA, and GA-TA microgels. (b) FT-IR spectra of linear GA, crosslinked GA microgel, GA-DETA microgel, and GA-TA microgels.

demonstrates the possible crosslinking of hydroxyl groups of GA with DVS. Approximate particle size of the prepared microgels was examined under optical microscope. The optical microscope images in Fig. 1b confirm that the microgels are spherical with variable microgel size ranges from 5 to 100 μM in hydrated state (upon swelling in DI water). For modification reactions, firstly the GA microgels were washed with NaOH for developing negative charges on the hydroxyl groups via deprotonation for further reaction with ECH, and modification agents such as DETA and TA

Fig. 2a and b give the schematic representation for modification of GA by DETA and TA respectively. In both cases initially the opening of the epoxy ring occurs followed by the addition of the modification agents.

Fig. 3a shows the distinctive color change of GA microgels after modification with DETA and TA respectively, which were obtained with relatively high yields e.g., 71 ± 3.1 for GA-DETA, and 67.4 ± 14.0% for GA-TA microgels. To verify chemical bonding between GA and DVS, Fourier Transform Infrared Spectrometry (FT-IR) of the prepared m microgels was recorded in the range 4000–650 cm^{-1} using FT-IR spectrometer. Fig. 3b shows the FT-IR spectra of linear and crosslinked GA. Both linear and crosslinked GA show a similar FT-IR pattern with the appearance of some new peaks for the sulfur-containing groups. The broad peak from 3500 cm^{-1} to 3100 cm^{-1} for GA and microgel confirms the excess of −OH groups on its surface (Li et al., 2009). Similarly, the specific peaks at 2934–2887, 1600, 1400 and 1032 cm^{-1} were attributed to —CH, —C═O, and —C—O groups of GA, respectively (Wang et al., 2014). The characteristic peaks at 1317 and 1285 cm^{-1} in crosslinked GA correspond to the S═O modes of linked sulfones which are in close agreement with literature values (Morales-Sanfrutos, Lopez-Jaramillo, Elremaily, Hernández-Mateo, & Santoyo-Gonzalez, 2015). Moreover, FT-IR spectra of modified GA microgel show successful pattern with new peaks confirming the surface modification of GA microgels. Fig. 3b shows comparison of FT-IR spectra of GA, GA-DETA and GA-TA microgels. In FT-IR spectrum of GA-DETA, the characteristic peaks near 3300, 1698 and 1654 cm^{-1} show −NH stretching frequency of amines that do not exist in bare GA microgels. Similarly the lower frequency peak at 1453 cm^{-1} confirms the C—N stretching vibrations for GA-DETA microgels (Song et al., 2015). In FT-IR spectrum of GA-TA microgels, the sharp peak at 1655 and the lower intensity shoulder at 1605 cm^{-1} is due to the formation of −NH and −C—N bounds after conjugation (Wu, Don, Lin, & Mi, 2014). The lower intensity peaks in the range from 1300 to 1200 cm^{-1} are due to the symmetric stretching vibrations of O═S═O.

GA microgels that have large particle size distributions were filtered through syringe filter with pore sizes of 5 μm initially to obtain a filtrate for smaller size of particles for DLS measurements. Table 1 represents the average diameter of GA, GA-DETA, and GA-TA microgels measured with DLS after filtration through 5 μm pore size syringe filter using DI water as solvent. As given in Table 1, the three-fold increase in size for GA-DETA microgels can be attributed to its highly positively-charged nature and swelling capability as compared to the negatively charged GA and GA-TA microgels. Average size distribution of GA, GA-TA, GA-DETA and GA-DETA-HCl are given in Supporting Fig. S1.

Surface charge can give adequate knowledge about modified material for use in the biomedical domain e.g., drug loading etc. To measure the apparent charge, the filtrated 5 μm pore size syringe filter GA, GA-DETA, and GA-TA and protonated GA-DETA microgels were subjected to zeta potential measurements after suspension in DI water. The cumulative negative charges for bare and TA modified microgels were −27.3 ± 4.2 and −24.8 ± 1.3 respectively. For modified GA-DETA microgel, a positive charge with approximate value of 5.2 ± 4.1 was recorded. Furthermore, modified GA-DETA-HCl showed 27 ± 15 surface charge upon protonation with 1 M HCl that may lead to high antibacterial activity. The apparent positive and negative charges on the microgel surface are due the new functional groups generated with the modification, such as OH, S═O and $^{+}NH_4$ for GA,GA-TA, and GA-DETA respectively (Akhlaghi et al., 2015; Pahlavanlu, Christensen, Therrien, & Wolf, 2015).

To determine the thermal stability after crosslinking GA microgels, TGA for linear and crosslinked GA was performed under nitrogen atmosphere with 100 mL/min flow rate with heating rate of 10 °C/min heating up to 900 °C. It is evident from Supporting Table 1, and Fig. 4a that linear GA show up to 5% weight loss in the first degradation step from 71 to 174 °C which is comparable with the weight loss for DVS crosslinked GA from 100 to 235 °C which confirm the evaporation of some water as solvent from GA (Banerjee & Chen, 2007; Jiang, Zhu, Yao, Fu, & Guan, 2012; Zohuriaan-Mehr, Motazedi, Kabiri, & Ershad-Langroudi, 2005). But in the second degradation step (25–200 °C) the weight loss for crosslinked GA show an increase up to 14.2 wt%, which manifests the complete removal of water from the gel (Wang, Sánchez-Soto, & Abt, 2016). A prominent change in the degradation profiles of linear and crosslinked GA is visible in the third degradation steps near 300 °C which exhibits the stability of DVS crosslinked GA over the linear GA and is sustained till the fourth degradation step. The total decrease in weight loss for GA microgel in comparison to linear GA sample seems to be 10% confirming the successful crosslinking of GA linear chains. Overlay of thermograms of GA, GA-DETA, and GA-TA microgels is shown in Fig. 4b.

Four prominent degradation ranges were observed for GA, GA-TA, and GA-DETA microgels, given in Supporting Table S1. Briefly, the comparison of the TGA curves for GA and GA-DETA microgels shows a nonlinear variation in weight loss. Till 200 °C, the alternate weight loss for both the GA and GA-DETA microgels is comparable; which justify the mechanism of evaporation of solvent followed by the dehydration of the gels (Banerjee & Chen, 2007), but soon after 220 °C it abruptly changes showing higher weight loss (50 wt%) for GA-DETA as shown by the dotted line in Fig. 3b. This increase in

Table 1
Zeta potential measurement, and particle size distribution via DLS for bare, modified, and protonated GA microgels.

Material	GA microgel	Modified GA-Taurine microgel	Modified GA-DETA microgel	Protonated GA-DETA-HCl microgel
DLS measurement (nm)	538 ± 37	523 ± 33	1531 ± 45	1640 ± 26
Zeta Potential (mV)	−27.3 ± 4.2	−24.8 ± 1.3	+5.2 ± 4.1	+27 ± 15

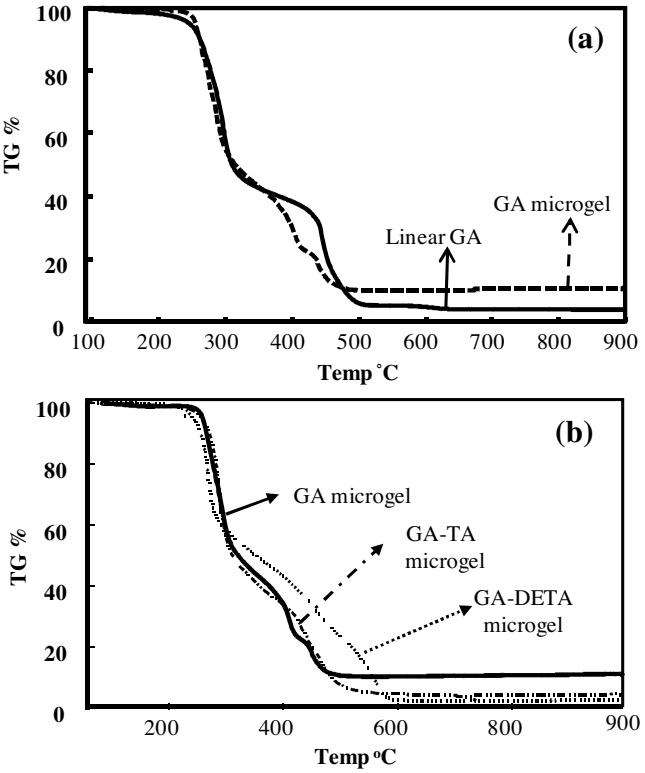

Fig. 4. TGA of (a) linear and DVS crosslinked GA microgel, and (b) ccomparison of tthermogram of GA, GA-DETA, and GA-TA microgels.

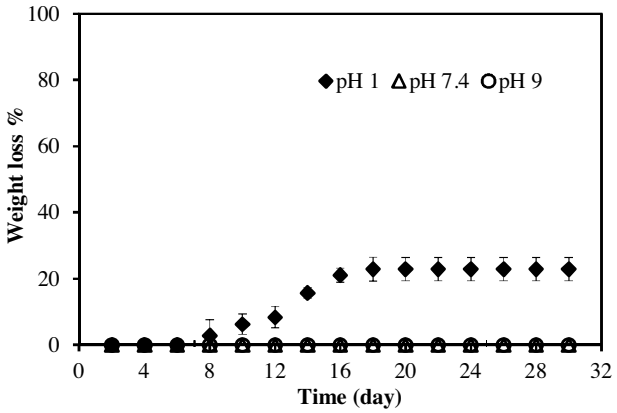

Fig. 5. The weight loss% of GA microgel at pH 1, pH 7.4, and pH 9 buffer solutions at 37.5 °C.

weight loss for GA-DETA may be attributed to the surface active amine groups (Huang, Zhou, & Han, 2013; McMinn, Matray, & Greenberg, 1997). Similar behavior was also observed in thermogram of GA-TA microgel. As can be seen from Table S1, the main decomposition steps of GA-TA microgel starts from a short temperature range of 245–313 °C. A gradual weight loss was recorded at the third and fourth decomposition steps which manifests the decomposition followed by the carbonization of GA-TA (Fan et al., 2015).

3.2. Hydrolytic degradation of GA microgels

The hydrolytic degradation study of GA microgels was carried out by using buffer solutions with three pH solutions and measured via HPLC methods. From the HPLC chromatogram of linear GA solution in DI water, the retention time of GA molecule was measured as 7.14 min, and the calibration of the GA solution was done for this peak at three different pHs. Hydrolytic degradation profiles of GA microgels were determined at pH 1 (stomach conditions), pH 7.4 (blood and body fluid conditions), and pH 9 (intestinal conditions) at 37.5 °C as shown in Fig. 5.

As can be seen from Fig. 5, there is no degradation observed within 8 days for each pH condition. However, the hydrolytic degradation started after 8 days and continued about up to 20 days with 22.8 ± 3.5% weight loss at pH 1 solution and there was no degradation was observed up to 30 days. This phenomenon is totally based upon the degree of crosslinking i.e., soon after addition of crosslinker during microgel synthesis some of the crosslinker molecules can directly crosslinks the GA polymer resulting in higher degree of crosslinking (Muzzarelli, 2009). On the other hand, with the passage of reaction time, the availability of free crosslinker molecules are decreased, hence the degree of crosslinking on periphery of GA microgels is lessen in comparison to the core of the microgels. In this study, the residue after 20 day of degradation profile confirms the presence of highly crosslinked GA microgels. Additionally, the degradation of GA microgel can be affected by the pH of the solution and it can degrade with a linear profile for a long time in stomach conditions in the body. The hydrolytic degradation process without enzyme is generally slow and takes longer time periods. Also, hydrolysis of crosslinked chains can be affected by the swelling ratio, pH conditions, temperature, and by the types and the degree of the crosslinkers. The degradation of microgels at different pH buffers can be correlated with the pH effects on hydrophilicity of the microgels (Sailema-Palate, Vidaurre, Campillo, & Castilla-Cortázar, 2016). The crosslinked GA microgel structure were more stable at neutral and basic conditions, whereas, some degradation was obtained at acidic condition with high swelling ratio.

3.3. Hemocompatibility of GA-based microgels

Biomaterials that may be used as biomedical devices can come in contact with blood and may affect the blood cells adversely and can change the coagulation and thrombosis mechanisms in the body. Therefore, the hemocompatibility of bare and modified GA microgels were determined for their further potential in the biomedical realm as blood contacting materials. In this experiment, GA, GA-DETA, and GA-TA microgels were subjected to *in vitro* tests for protein adsorption, % hemolysis ratio and blood clotting index. The obtained data is given in Fig. 6a, b, and c, respectively. Adsorption of plasma protein on the prepared microgels is a very important parameter for hemocompatibility of materials with potential in biomedical field. BSA (Model protein) adsorption amounts (mg/g) of bare GA, GA-DETA, and GA-TA were measured as 110 ± 20, 169 ± 18, and 102 ± 19 mg/g BSA, respectively as presented in Fig. 6a.

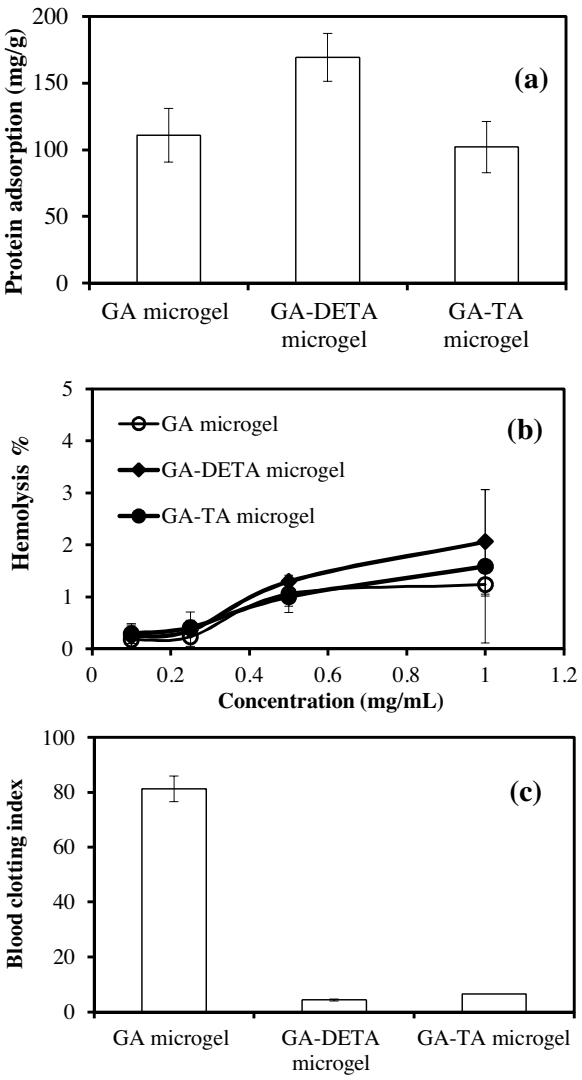

Fig. 6. (a) Protein (BSA) adsorption (mg/g), (b) hemolysis%, and (c) blood clotting index results of bare GA, GA-DETA, and GA-TA microgels.

The highest protein adsorption was observed for modified GA-DETA microgels which can be attributed to its positive surface charges and more hydrophilicity compared with the other GA and GA-TA microgels. High variations in the standard deviation of the protein adsorption values can be attributed to the large size distribution and degree of crosslinker as well as the differences in the porosity of the microgels of the different sizes. Hemolysis, the destruction of erythrocyte cells, is another important aspect for hemocompatibility for the evaluation of blood contacting devices. Owing to the standard classification; 0–2%, 2–5%, and 5–100% hemolysis are non-hemolytic, slightly hemolytic, and hemolytic material, respectively (Li et al., 2015). The percent hemolysis ratios for GA, GA-DETA, and GA-TA microgels were $1.2 \pm 0.2\%$, $2.0 \pm 1.4\%$, and $1.5 \pm 1.0\%$, respectively at 1 mg/mL concentration as shown in Fig. 6b. These results clearly revealed that bare GA microgel were non-hemolytic, whereas, modified GA microgels were slightly hemolytic materials.

Modifications do not retard the hemolytic mechanism in the blood, and the use of bare and modified microgels can be considered as safe for blood contacting devices. The other significant parameter is the change of coagulation and thrombosis mechanisms of blood upon contacting with biomaterials. Blood clotting index values of GA, GA-DETA, and GA-TA microgels at 1 mg/mL concentration were found as 81 ± 5, 4 ± 1, and 6 ± 4, respectively as shown in Fig. 6c. These results directly indicate that GA microgel is also safe and can be considered as benevolent materials for blood contacting devices, whereas modified GA microgels induced the clotting mechanism in blood.

3.4. Cell viability, apoptotic and necrotic assay of bare and modified GA microgels

The biocompatibility of GA-based microgels was tested against L929 fibroblast cells. The histograms in Fig. 7 present the cell viability, apoptosis and necrosis percent values for L929 fibroblast cells using bare and modified GA microgels at nutritious dosages in various concentrations ranging from 1 to 200 μg/mL. The results in Fig. 7a clearly demonstrate the optimized concentration for% cell viability as 25 μg/mL, which resulted in 84.4%, 89.1%, and 67.04% cell viability for GA, GA-DETA, and GA-TA microgels, respectively.

The relatively high cell viability for GA-DETA is attributed to surface amine groups that can contribute to the enhancement of biocompatibility of microgels (Akhlaghi et al., 2015). Apoptosis percent activity of bare and modified (GA-DETA and GA-TA) GA microgels increases with the increase in the concentrations in a linear manner. A comparatively high apoptotic activity was recorded for GA-TA microgels (44%) at 200 μg/mL concentration as illustrated in Fig. 7b and their fluorescent microscope images are given in Fig. 7d. It is clearly seen from the images that the blue color of cell nuclei for control was changed to bright blue which comes from apoptotic cells at 100 μg/mL concentration for GA-TA. Addition of TA functional groups into the mitochondria-driven apoptotic mechanism readily reduced intracellular calcium level which suppresses the induction of the mitochondrial permeability transition (mPT) by inhibiting the opening of mitochondrial permeability transition pores (Chen et al., 2009).

L929 Fibroblast cells were also subjected to necrotic effect after mixing with various amounts of GA, GA-DETA and GA-TA microgels. The intensity of the bars given in Fig. 7c indicates that the necrotic ratio for bare GA microgels is negligible at low dosage amounts but almost linearly increases at 50 to 200 μg/mL concentrations. The highest necrotic activity for bare GA microgels was found out to be 28% at 200 μg/mL dosage. For modified GA microgel (GA-DETA and GA-TA) the necrotic effects were also linearly increased with increasing dosage. The recorded necrotic ratios were 21 and 18% for GA-DETA and GA-TA microgels at 200 μg/mL concentration. Moreover, the necrotic cell images of L929 fibroblast cells were illustrated in Fig. 7e. The necrotic cell nuclei at 100 μg/mL concentration of GA-TA microgels look red stained as demonstrated with arrow.

3.5. Antimicrobial effects of GA-based microgel

E. coli (gram −) and *S. aureus* (gram +) were used as model microorganisms to determine antimicrobial effects of GA-based microgels after the modification and protonation reactions. Antimicrobial susceptibility of GA, GA-TA, GA-DETA, and protonated GA-DETA microgels were investigated against *E. coli and S. aureus* and there are no killing effects was obtained for GA, GA-TA, and GA-DETA. Minimum inhibition concentration (MIC) values for protonated GA-DETA microgel were found to be 5 mg/mL and 10 mg/mL against *E. coli* and *S. aureus*, respectively. Digital camera images for stock solutions and MIC of protonated GA-DETA microgels spread on agar plates were also demonstrated in Supporting Fig. S2. The protonated GA-DETA microgel can prevent bacterial growth against each bacteria strains such as (gram + and gram −), whereas, bare GA and only GA microgel modified with TA and DETA show negligible bactericidal effects against the microorganisms. Moreover, protonated GA-DETA microgels were highly suscepti-

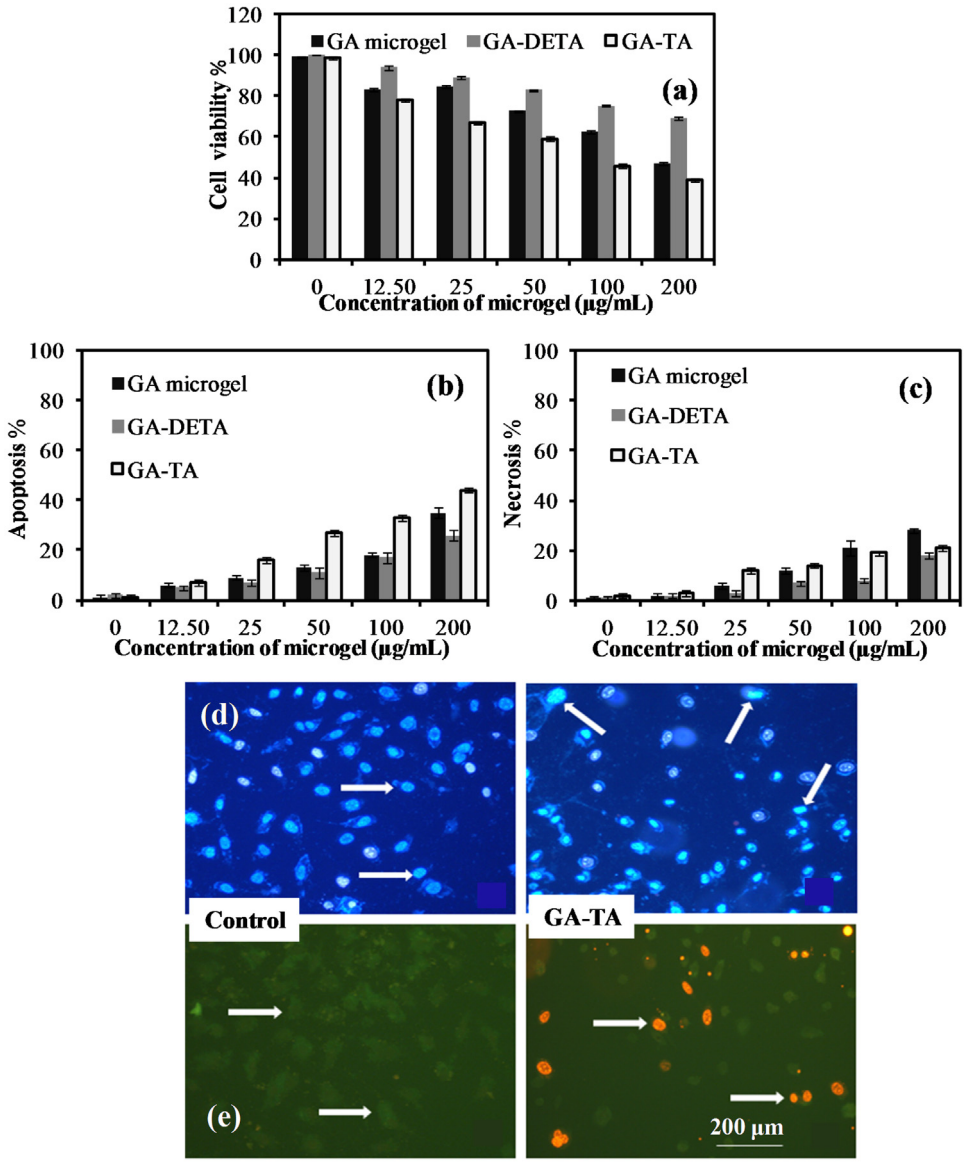

Fig. 7. (a) Cell viability%, (b) apoptosis%, and (c) necrosis% of bare GA, GA-DETA, and GA-TA microgels against L929 fibroblast cells. Fluorescent microscope images of (d) apoptotic and (e) necrotic L929 fibroblast cells for control, and 100 μg/mL concentration of GA-TA microgel by using double staining performed with Hoechst 33342 and propidium iodide (PI) fluorescent strains. Photographs were taken by Lecia DMI 600 fluorescent microscope at 200× magnification.

ble against *E. coli* compared to *S. aureus* strains related to their highly positive charge (+27 ± 15 mV of zeta potential). Therefore, the GA microgels are very useful and versatile as they can even form antibacterial material by chemical modifications while they are considered biocompatible in their unmodified forms. The changes in the swelling/deswelling values and liquid uptake behavior of GA microgels following their DETA and TA derivatization will be investigated in the future studies.

4. Conclusions

This preliminary study shows a one-pot route for the synthesis of GA microgels via water-in-oil micro-emulsion polymerization technique with a high yield of 78.5 ± 5.0%. The as prepared GA microgels have superficial hydroxyl groups which gives −27.31 ± 4.2 mV overall surface charge. GA microgels were further modified with DETA and TA to have different functional groups, and it was shown that GA microgels can render a surface charge up to +27 ± 15 mV for additional characteristics such as bactericidal properties. Similarly, GA microgels show 22.8 ± 3.5 biodegradability property at stomach condition (pH 1) in 20 days. Moreover, GA, GA-DETA and GA-TA microgels exhibit high hemocompatibility with high protein adsorption capacity, low hemolysis effects for blood and possess low apoptotic and neurotic indices up to 50 μg/mL. Furthermore, the protonated DETA modified GA show a pronounced killing effect against gram negative and gram positive bacteria species. Therefore, bare and modified GA microgels can be used as bio-devices for potential biological applications with their tunable chemical and physical properties with various size and surface charges via chemical modification prepared as reported here can be considered as multipurpose material with biological origin and great potential in biomedical field.

Acknowledgements

M. Farooq is grateful to The Scientific and Technological Research Council of Turkey (TUBITAK) for the support under the TUBITAK 2216 research fellowship program.

Appendix A. Supplementary data

Supplementary data associated with this article can be found, in the online version, at http://dx.doi.org/10.1016/j.carbpol.2016.09.052.

References

Akhlaghi, S. P., Zaman, M., Mohammed, N., Brinatti, C., et al. (2015). Synthesis of amine functionalized cellulose nanocrystals: Optimization and characterization. *Carbohydrate Research*, *409*, 48–55.

Ali, A. A., Ali, K. E., Fadlalla, A. E., & Khalid, K. E. (2008). The effects of gum arabic oral treatment on the metabolic profile of chronic renal failure patients under regular haemodialysis in Central Sudan. *Natural Product Research*, *22*(1), 12–21.

An, F., An, Q., Bai, J., Balantekin, A., Band, H. R., et al. (2013). Improved measurement of electron antineutrino disappearance at Daya Bay. *Chinese Physics C*, *37*(1), 011001.

Anirudhan, T., & Rauf, T. A. (2013). Adsorption performance of amine functionalized cellulose grafted epichlorohydrin for the removal of nitrate from aqueous solutions. *Journal of Industrial and Engineering Chemistry*, *19*(5), 1659–1667.

Archana, D., Dutta, J., & Dutta, P. (2013). Evaluation of chitosan nano dressing for wound healing: Characterization, in vitro and in vivo studies. *International Journal of Biological Macromolecules*, *57*, 193–203.

Banerjee, S. S., & Chen, D.-H. (2007). Fast removal of copper ions by gum arabic modified magnetic nano-adsorbent. *Journal of Hazardous Materials*, *147*(3), 792–799.

Bhardwaj, T. R., Kanwar, M., Lal, R., & Gupta, A. (2000). Natural gums and modified natural gums as sustained-release carriers. *Drug Development and Industrial Pharmacy*, *26*(10), 1025–1038.

Chen, K., Zhang, Q., Wang, J., Liu, F., et al. (2009). Taurine protects transformed rat retinal ganglion cells from hypoxia-induced apoptosis by preventing mitochondrial dysfunction. *Brain Research*, *1279*, 131–138.

Ciofani, G., Del Turco, S., Rocca, A., De Vito, G., Cappello, V., Yamaguchi, M., et al. (2014). Cytocompatibility evaluation of gum Arabic-coated ultra-pure boron nitride nanotubes on human cells. *Nanomedicine*, *9*(6), 773–788.

Comte, S., Guibaud, G., & Baudu, M. (2008). Biosorption properties of extracellular polymeric substances (EPS) towards Cd, Cu and Pb for different pH values. *Journal of Hazardous Materials*, *151*(1), 185–193.

Crayton, P. H., Zitomer, F., & Lambert, J. (1963). Inner complexes of cobalt (III) with diethylenetriamine. *Inorganic Syntheses, Vol. 7*, 207–213.

de las Heras Alarcón, C., Pennadam, S., & Alexander, C. (2005). Stimuli responsive polymers for biomedical applications. *Chemical Society Reviews*, *34*(3), 276–285.

Dwivedi, A. D., Dubey, S. P., Hokkanen, S., Fallah, R. N., & Sillanpää, M. (2014). Recovery of gold from aqueous solutions by taurine modified cellulose: An adsorptive-reduction pathway. *Chemical Engineering Journal*, *255*, 97–106.

Ekici, S., Ilgin, P., Butun, S., & Sahiner, N. (2011). Hyaluronic acid hydrogel particles with tunable charges as potential drug delivery devices. *Carbohydrate Polymers*, *84*(4), 1306–1313.

Erdem, H. O., & Bicak, N. (2016). Preparation of PANI coated polymer microspheres and their use as Michael acceptor for direct immobilization of amines and amino acids. *Reactive and Functional Polymers*, *99*, 88–94.

Fan, Y., Liu, P., Zhu, B., Chen, S., Yao, K., & Han, R. (2015). Microporous carbon derived from acacia gum with tuned porosity for high-performance electrochemical capacitors. *International Journal of Hydrogen Energy*, *40*(18), 6188–6196.

Ganie, S. A., Ali, A., & Mazumdar, N. (2015). Iodine derivatives of chemically modified gum Arabic microspheres. *Carbohydrate Polymers*, *129*, 224–231.

Huang, M.-X., Zhou, C.-R., & Han, X.-W. (2013). Investigation of thermal decomposition kinetics of taurine. *Journal of Thermal Analysis and Calorimetry*, *113*(2), 589–593.

Ilgin, P., Avci, G., Silan, C., Ekici, S., Aktas, N., Ayyala, R. S., et al. (2010). Colloidal drug carries from (sub) micron hyaluronic acid hydrogel particles with tunable properties for biomedical applications. *Carbohydrate Polymers*, *82*(3), 997–1003.

Irving, C. S., Hammer, B. E., Danyluk, S. S., & Klein, P. D. (1980). 13C Nuclear magnetic resonance study of the complexation of calcium by taurine. *Journal of Inorganic Biochemistry*, *13*(2), 137–150.

Jegelka, M., & Plietker, B. (2012). Dual catalysis: Vinyl sulfones through tandem iron-catalyzed allylic sulfonation amine-catalyzed isomerization. *ChemCatChem*, *4*(3), 329–332.

Jiang, R., Zhu, H., Yao, J., Fu, Y., & Guan, Y. (2012). Chitosan hydrogel films as a template for mild biosynthesis of CdS quantum dots with highly efficient photocatalytic activity. *Applied Surface Science*, *258*(8), 3513–3518.

Li, X., Chen, S., Hu, W., Shi, S., Shen, W., Zhang, X., et al. (2009). In situ synthesis of CdS nanoparticles on bacterial cellulose nanofibers. *Carbohydrate Polymers*, *76*(4), 509–512.

Li, R., Wu, G., & Ye, Y. (2015). In vitro hemocompatibility of sulfonated polypropylene non-woven fabric prepared via a facile γ-ray pre-irradiation grafting method. *Applied Surface Science*, *356*, 1221–1228.

Liimatainen, H., Sirviö, J., Pajari, H., Hormi, O., & Niinimäki, J. (2013). Regeneration and recycling of aqueous periodate solution in dialdehyde cellulose production. *Journal of Wood Chemistry and Technology*, *33*(4), 258–266.

Malviya, N., Jain, S., & Malviya, S. (2010). Antidiabetic potential of medicinal plants. *Acta Poloniae Pharmaceutica*, *67*(2), 113–118.

Mather, B. D., Viswanathan, K., Miller, K. M., & Long, T. E. (2006). Michael addition reactions in macromolecular design for emerging technologies. *Progress in Polymer Science*, *31*(5), 487–531.

McMinn, D. L., Matray, T. J., & Greenberg, M. M. (1997). Efficient solution phase synthesis of oligonucleotide conjugates using protected biopolymers containing 3'-terminal alkyl amines. *The Journal of Organic Chemistry*, *62*(21), 7074–7075.

Morales-Sanfrutos, J., Lopez-Jaramillo, J., Ortega-Muñoz, M., Megia-Fernandez, A., Perez-Balderas, F., Hernandez-Mateo, F., et al. (2010). Vinyl sulfone: A versatile function for simple bioconjugation and immobilization. *Organic & Biomolecular Chemistry*, *8*(3), 667–675.

Morales-Sanfrutos, J., Lopez-Jaramillo, F. J., Elremaily, M. A., Hernández-Mateo, F., & Santoyo-Gonzalez, F. (2015). Divinyl sulfone cross-linked cyclodextrin-based polymeric materials: Synthesis and applications as sorbents and encapsulating agents. *Molecules*, *20*(3), 3565–3581.

Muzzarelli, R. A. (2009). Genipin-crosslinked chitosan hydrogels as biomedical and pharmaceutical aids. *Carbohydrate Polymers*, *77*(1), 1–9.

Ngah, W. W., Teong, L., & Hanafiah, M. (2011). Adsorption of dyes and heavy metal ions by chitosan composites: A review. *Carbohydrate Polymers*, *83*(4), 1446–1456.

Oh, J. K., Lee, D. I., & Park, J. M. (2009). Biopolymer-based microgels/nanogels for drug delivery applications. *Progress in Polymer Science*, *34*(12), 1261–1282.

Pahlavanlu, P., Christensen, P. R., Therrien, J. A., & Wolf, M. O. (2015). Controlled intramolecular charge transfer using a sulfur-containing acceptor group. *The Journal of Physical Chemistry C*,

Phillips, G., & Williams, P. (2001). Tree exudate gums: Natural and versatile food additives and ingredients. *Food Ingredients and Analysis International*, 26.

Pologanathan, K., & Mahendran, M. (2012). Shear tests of lipped channel beams with stiffened web openings. From Materials to Structures: Advancement through Innovation. *Proceedings of the 22nd australasian conference on the mechanics of structures and materials*, 819–824. CRC Press.

Romo-Hualde, A., Yetano-Cunchillos, A., González-Ferrero, C., Sáiz-Abajo, M., & González-Navarro, C. (2012). Supercritical fluid extraction and microencapsulation of bioactive compounds from red pepper (*Capsicum annum* L.) by-products. *Food Chemistry*, *133*(3), 1045–1049.

Sagbas, S., Butun, S., & Sahiner, N. (2012). Modifiable chemically crosslinked poli (κ-carrageenan) particles. *Carbohydrate Polymers*, *87*(4), 2718–2724.

Sahiner, N., & Xinqiao, J. (2008). One-step synthesis of hyaluronic acid-based (sub) micron hydrogel particles: Process optimization and preliminary characterization. *Turkish Journal of Chemistry*, *32*(4), 397–409.

Sahiner, N., Sagbas, S., & Turk, M. (2014). Poly (sucrose) micro particles preparation and their use as biomaterials. *International Journal of Biological Macromolecules*, *66*, 236–244.

Sahiner, N., Sagbas, S., & Aktas, N. (2016). Preparation of macro-, micro-: and nano-sized poly (Tannic acid) particles with controllable degradability and multiple biomedical uses. *Polymer Degradation and Stability*, *129*, 96–105.

Sailema-Palate, G. P., Vidaurre, A., Campillo, A., & Castilla-Cortázar, I. (2016). A comparative study on Poly (ε-caprolactone) film degradation at extreme pH values. *Polymer Degradation and Stability*.

Sardo, C., Farra, R., Licciardi, M., Dapas, B., et al. (2015). Development of a simple: Biocompatible and cost-effective Inulin-Diethylenetriamine based siRNA delivery system. *European Journal of Pharmaceutical Sciences*, *75*, 60–71.

Sarika, P., & James, N. R. (2015). Preparation and characterisation of gelatin-gum arabic aldehyde nanogels via inverse miniemulsion technique. *International Journal of Biological Macromolecules*, *76*, 181–187.

Schmuhl, R., Krieg, H., & Keizer, K. (2004). Adsorption of Cu (II) and Cr (VI) ions by chitosan: Kinetics and equilibrium studies. *Water Sa*, *27*(1), 1–8.

Shih, M.-F., Shau, M.-D., Chang, M.-Y., Chiou, S.-K., Chang, J.-K., & Cherng, J.-Y. (2006). Platelet adsorption and hemolytic properties of liquid crystal/composite polymers. *International Journal of Pharmaceutics*, *327*(1), 117–125.

Song, Z. X., Li, W., Liu, W. T., Yang, Y., Wang, N. N., Wang, H. J., et al. (2015). Novel magnetic lignin composite sorbent for chromium(VI) adsorption. *Rsc Advances*, *5*(17), 13028–13035.

Venault, A., Trinh, K. M., & Chang, Y. (2016). A zwitterionic zP (4VP-r-ODA) copolymer for providing polypropylene membranes with improved hemocompatibility. *Journal of Membrane Science*, *501*, 68–78.

Verbeken, D., Dierckx, S., & Dewettinck, K. (2003). Exudate gums: Occurrence, production, and applications. *Applied Microbiology and Biotechnology*, *63*(1), 10–21.

Wang, T., Liu, Q., Li, G., Xu, K., Zou, R., & Hu, J. (2014). Hydrothermal control growth of Zn 2 GeO 4-diethylenetriamine 3D dumbbell-like nanobundles. *CrystEngComm*, *16*(15), 3222–3227.

Wang, L., Sánchez-Soto, M., & Abt, T. (2016). Properties of bio-based gum Arabic/clay aerogels. *Industrial Crops and Products*, *91*, 15–21.

Wu, S.-J., Don, T.-M., Lin, C.-W., & Mi, F.-L. (2014). Delivery of berberine using chitosan/fucoidan-taurine conjugate nanoparticles for treatment of defective intestinal epithelial tight junction barrier. *Marine Drugs*, *12*(11), 5677–5697.

Zohuriaan-Mehr, M. J., Motazedi, Z., Kabiri, K., & Ershad-Langroudi, A. (2005). New Super-absorbing hydrogel hybrids from gum arabic and acrylic monomers. *Journal of Macromolecular Science, Part A*, *42*(12), 1655–1666.